CHAPTER SEVEN

EXPERIMENTAL RESULTS

EFFECT OF THE STEEL'S COMPOSITION

7.1 EFFECT OF ANNEALING TREATMENT ON STEEL B

In order to understand the precipitation behaviour of the Laves phase more precisely, an AISI type 441 (Steel B (0.149%Ti-0.445Nb-0.008%Mo)) that did not fail during processing was used. The Charpy impact specimens from this steel were annealed at temperatures between 850 °C and 950 °C for 30 minutes followed by quenching into water. The quantity of precipitates in the steel after annealing was then electrolytically extracted and the volume fraction of Laves phase was measured and calculated through powder XRD. The results in Figure 7.1 show that after annealing at 850 °C, the amount of Laves phase has decreased to about 0.13% from the 0.2% in the as received condition, and annealing at 950 °C, a further decrease to about 0.05% occurred. A small remnant of Laves phase of about 0.05% volume fraction was still found in this steel, even after annealing at the temperature of 950 °C. This contrasts with the calculated solvus temperature of about 800 °C as was found by Thermo-Calc® for this particular steel.

The Charpy impact tests, however, reveal that after annealing at 850 °C, the remaining quantity of Laves phase of about 0.15% does not reduce the CIE as significantly as did the larger Laves phase volume fraction of 0.2% on the grain boundaries upon hot rolling in the as received material. In this particular steel it, therefore, appears that a critical maximum volume fraction of Laves phase that may avoid significant impact embrittlement is about 0.15% although this particular value may also depend on the size of the Laves phase particles on the grain boundaries and on the precise alloy composition. With annealing at 950 °C, grain growth starts to affect the CIE value and the very small volume fraction of about 0.05% of remaining Laves phase is probably insignificant.

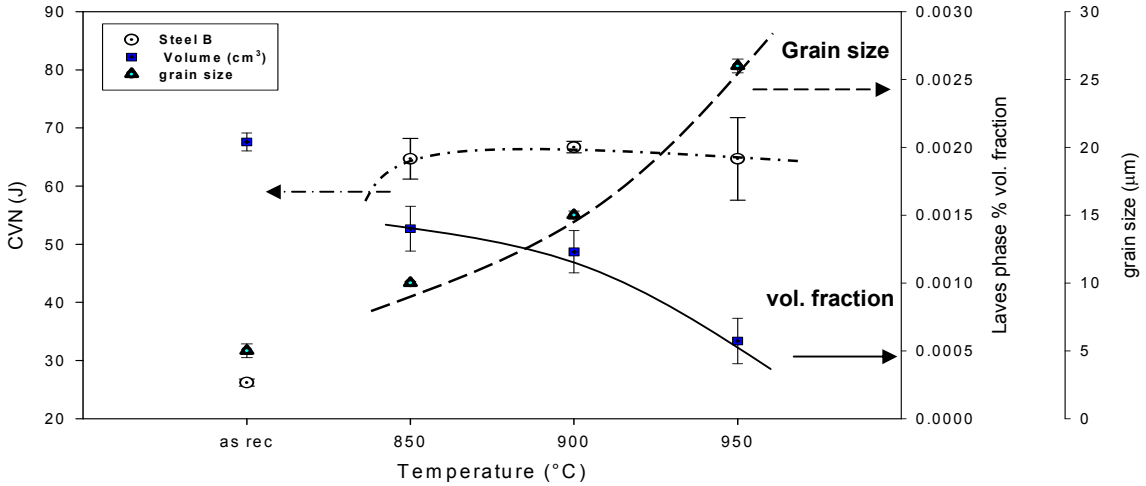

Figure 7.1. Effect of annealing treatment on the Laves phase's % volume fraction, grain size and the Charpy impact toughness of the 441 ferritic stainless steel, Steel B.

7.2 Effect of the Equilibrium Laves Phase Volume Fraction on the Room Temperature Charpy Impact Energy

In the above experiment discussed in Section 7.1, a constant annealing time of 30 minutes was used at various temperatures to vary the volume fraction of the Laves phase, i.e. at lower temperatures it may be that equilibrium conditions had not been fully achieved. A second set of Charpy specimens was then used with annealing at a constant temperature of 800 °C but with now varying the time to study any possible effects of achieving or not achieving equilibrium conditions in the Laves phase formation. The Charpy impact specimens were, therefore, heated at 800 °C for a period of between 5 minutes and 300 minutes followed by quenching into water and then the quantity of the Laves phase precipitates was measured. The results are given in Figure 7.2, which show that in the as received hot rolled material which had a relatively high volume fraction of about 0.2% of Laves phase, this had resulted in lowering the CIE to about 25 J, and after annealing at 800 °C for 5 minutes, 33% of the Laves phase had already dissolved in this steel and this resulted in a large improvement in its CIE to above 50 J. Further annealing periods did improve the CIE only marginally to about 60 J. It, therefore, appears that equilibrium conditions are neared relatively quickly in the first few minutes of annealing at 800 °C with only a small time dependence after longer annealing times.

Considering the change in volume fraction in Figure 7.2 it appears that the dissolution of the slightly more than 0.2% Laves phase in the starting or as received material, takes place very rapidly with only about 0.07% left after 5 minutes at 800 °C. A very small degree of "overshoot" then seems to take place in the dissolution rate before equilibrium is established after 30 to 60 minutes at 800 °C. The reasons for such an "overshoot" are not quite clear but it would clearly fall into a non-equilibrium transient process. The very rapid dissolution rate in the first 5 minutes is even more remarkable if one considers that the heating up time within these first few minutes of the 5 mm thick specimens, should really be discounted from these first 5 minutes.

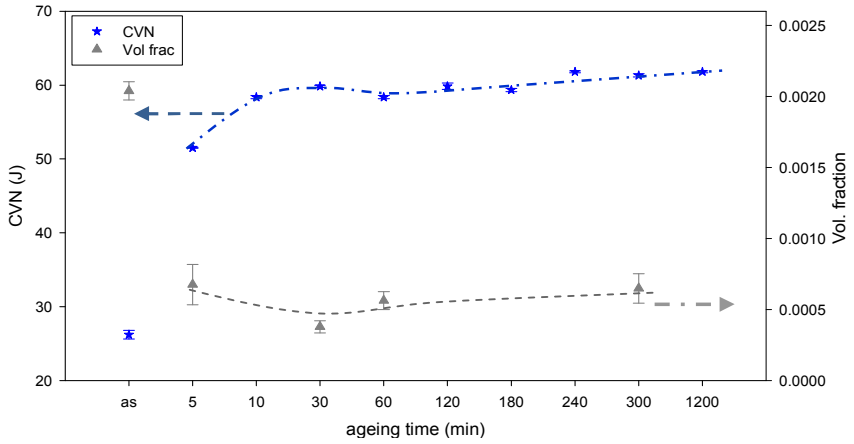

Figure 7.2. Effect of the Laves phase precipitation kinetics on the Charpy impact toughness of Steel B.

Comparing the CIE values in this Steel B with the earlier reported ones for Steel A in Chapter 6, it is surprising that there is only about 14 J difference in the CIE between the two as received hot rolled materials as processed by Columbus with Steel A rejected by Columbus due its CIE of only about 10 to 11 J and Steel B's 25 J which was accepted by Columbus. Microstructural analysis, however, revealed that Steel B had a much finer grain size than Steel A, and this may have resulted in the higher CIE for Steel B.

Figure 7.3 shows the optical microstructural evolution of Steel B in the as received hot rolled condition and after annealing treatments at different temperatures ranging from 850 to 950 °C. The as received microstructure in Figure 7.3(a) appears to be a partly dynamically recrystallised microstructure or alternatively, a post-rolling statically recrystallised microstructure with some recrystallised grains in an overwhelmingly unrecrystallised microstructure. Note furthermore, that recovery appears to have taken place primarily during static annealing at 850 °C with full recrystallisation only occurring at temperatures of 900 to 950 °C.

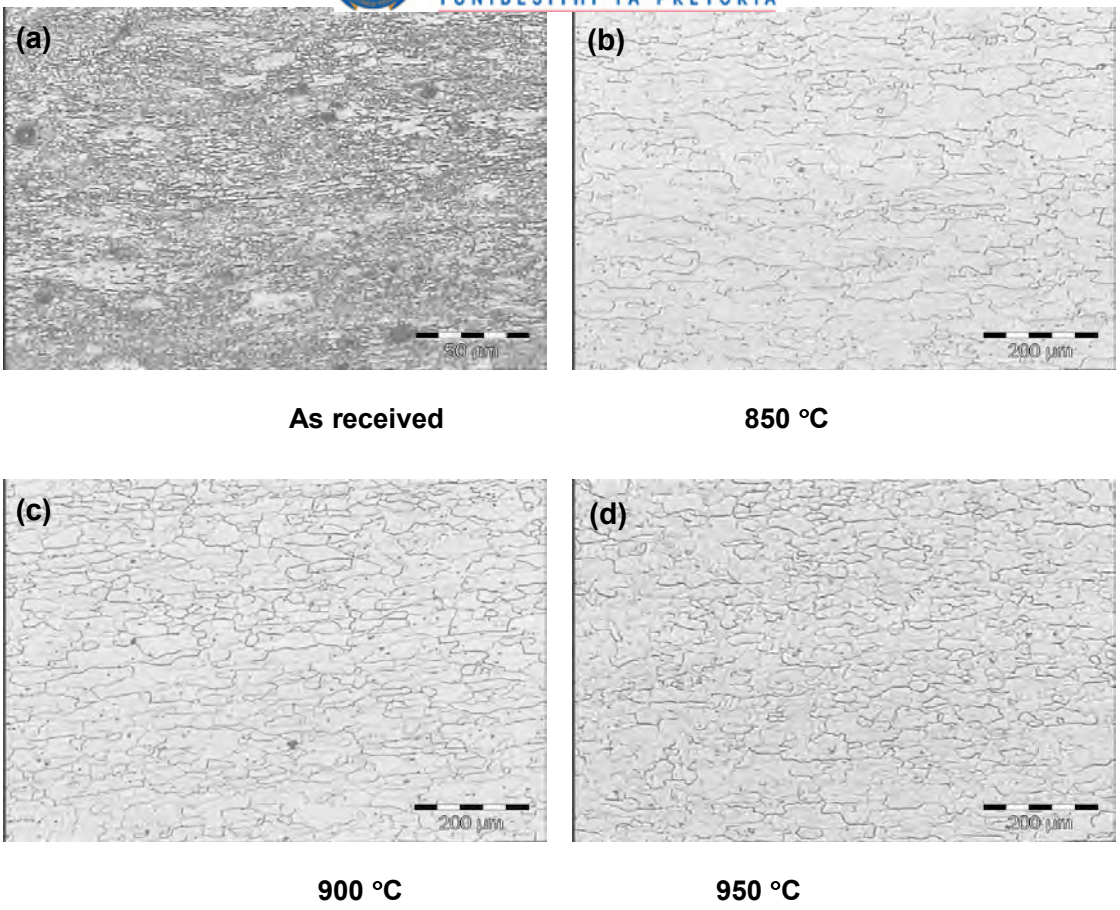

Figure 7.3. Optical micrographs of the specimens from steel B in the (a) as received plant hot rolled condition and (b) to (d) after being annealed at different temperatures from 850 to 950°C for 30 minutes followed by water quenching.

7.3 Effect of Annealing Treatment on the Embrittlement of the Experimental Stainless Steels C to E

Figure 7.4 shows the Charpy impact toughness behaviours of Steels C to E as a function of annealing treatment. These alloys are brittle over a very wide range of temperatures with the toughness's averaging below 5 J. It should be noted that some of these results from Steel C (0.36%Nb – 0.171%Ti - <0.01%Mo alloy, i.e. higher in Ti and lower in Nb than the commercial Steels A and B) are scatted between roughly two extremes; i.e. specimens of this steel are either entirely brittle or entirely ductile. Steels D (0.54%Mo) and E (1.942%Mo) are the molybdenum containing steels and they have shown very similar brittle behaviour. This suggests that any Mo additions to a AISI 441 type stainless steel has a negative impact on the toughness of this alloys, no doubt due to the expected higher volume fractions of Laves phase as predicted earlier in Chapter 5 by Thermo – Calc®. Comparing the CIEs of Steel C (Mo-free) to those of the Mo-

containing Steels D and E, it can be seen that Steel C had a much higher CIE at a number of annealing temperatures than the other two steels, although at some temperatures this was not the case where Steel C was equally brittle to Steels D and E. Again, this can be related to the quantity of Laves phase in Steel C, as it was previously shown by Thermo-Calc® predictions (see, Chapter 5.) that the Laves phase volume fraction in this steel should be much lower than in Steels D and E. Any Mo additions to a type 441 ferritic stainless steel should, therefore, be avoided.

Secondly, comparing the somewhat erratic CIE behaviour of Steel C (lower Nb and higher Ti contents) with annealing to the more consistent behaviour of the two commercial Steels A and B, one may conclude that lowering the Nb content and raising the Ti content in the dual stabilisation from the standard dual stabilisation, should be carefully considered in practice as it may have negative consequences. This tentative conclusion is, however, somewhat uncertain as these experimental steels also had a much larger grain size (see below) than the two commercial steels and some further studies could be considered to fully prove or disprove this tentative conclusion. The initial observation of the microstructure of the laboratory hot rolled experimental Steels C, D and E prior to any annealing treatment, showed them to have much larger grain sizes, typically more than 150 μm if compared to the plant hot-rolled materials in Steels A and B, see Figure 7.5. The effect of grain size on the toughness of ferritic stainless steels has been well documented over the years, and it is known that a large grain size decreases the toughness of the steel significantly. Because of the larger grain sizes than expected, no further work was done on the brittle behaviour of these three steels although they were still included in the studies to determine the effect of composition on the nucleation and kinetic precipitation behaviour of the Laves phase in these alloys.

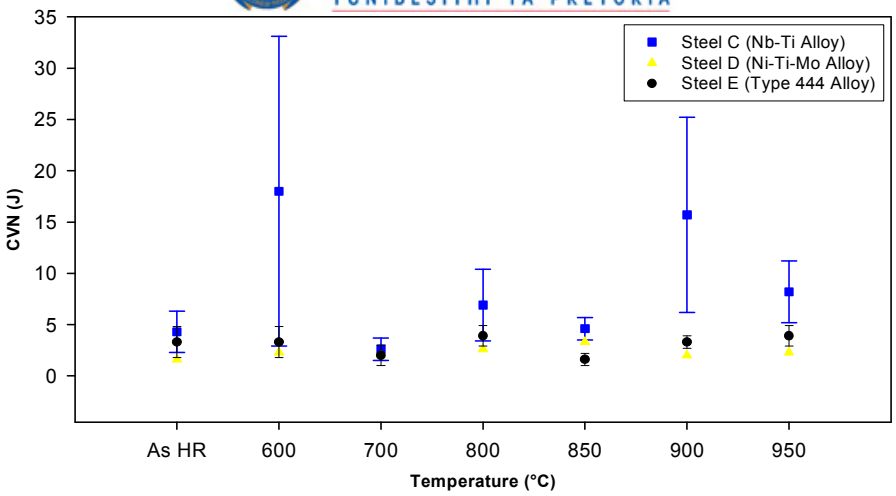

Figure 7.4. Effect of annealing temperature on the room temperature Charpy impact energy of the laboratory hot rolled materials. The samples were annealed for 30 minutes at different temperatures and then water quenched: Steel C (Nb-Ti alloy); Steel D (Nb-Ti-Mo alloy) and Steel E (Type 444 alloy).

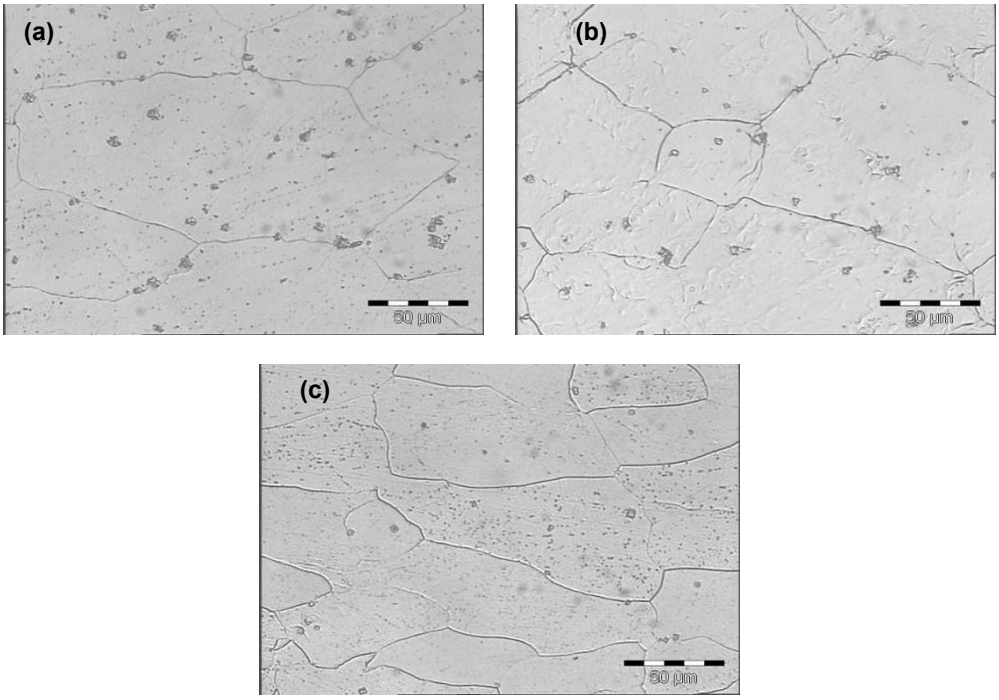

Figure 7.5. The microstructure of the laboratory hot-rolled experimental steels, showing different grain size distributions if compared to those of the commercial Steels A and B: (a) Steel C; (c) Steel D; and (d) Steel E.

CHAPTER EIGHT

EXPERIMENTAL RESULTS

LAVES PHASE KINETICS STUDY

8.1 INTRODUCTION

One of the most important aspects of this research work was to study the transformation kinetics of the Laves phase, in particular its nucleation and the overall volume fraction evolution. The research, therefore, focused on determining the Laves phase volume fraction as a function of time during annealing below 850 °C and this produced a frequently found sigmoidal or S–shaped curve. The transformation kinetics are then described using the well known Johnson–Mehl–Avrami–Kolmogorov (JMAK) type of equations [95]. The following parameters that affect the kinetics of the Laves phase precipitation were considered: annealing temperature and time, the alloy's and Laves phase's composition and the steel's grain size.

8.2 EQUILIBRIUM LAVES PHASE FRACTION

Thermo-Calc® software was first used to estimate the equilibrium Laves phase fraction in Steel A, as a function of temperature, see Chapter 5. All the possible phases, including the carbo-nitrides, were included in the calculations. The equilibrium fraction of the Laves phase as it was formed after long time annealing was then determined experimentally from the Steel A, i.e. the steel which had failed during production. The materials were first annealed at 850 °C for 2 hours in order to dissolve and minimise the Laves phase content and at the same time making sure that there was minimal grain growth, and the material was then quenched into water. The specimens where then annealed at temperatures between 600 and 850 °C for periods ranging from 5 to 1000 minutes and then water quenched. The precipitate residues where electrolytically extracted and analysed from these annealed specimens using XRD techniques. The physical quantity of the precipitates was determined from the relative intensity of XRD lines using a Rietveld technique, which enables the volume fraction – time relationship to be found with fair accuracy. Figure 8.1 shows the typical S-shaped curves plotted from these analyses. Note that the XRD analyses give the fractions in weight fraction, and these values had to be converted to volume fractions using the densities of each phase

and using the overall weighed amount of the precipitate residues collected. An example of such a calculation was shown in Section 6.2.1 and the overall results are shown in Figure 8.1.

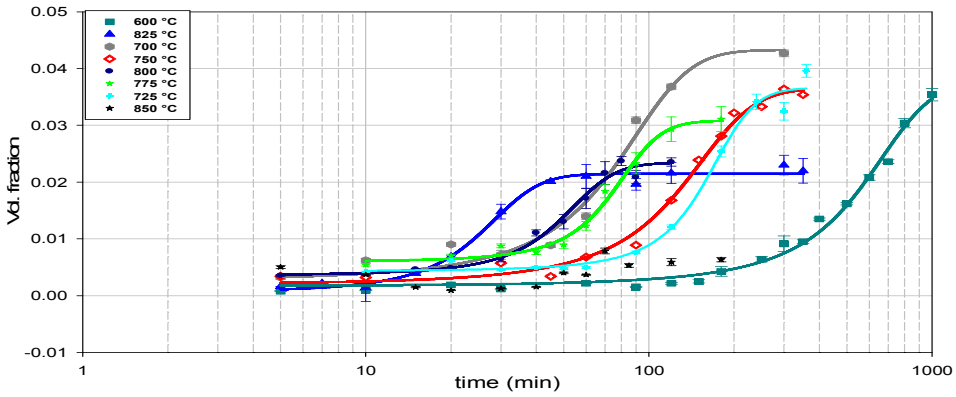

Figure 8.1. The Laves phase volume fraction – temperature/time curves during isothermal annealing in the temperature range 600 °C to 850 °C.

From Figure 8.1, it was observed that for the specimens that were heated at 600 °C, even after annealing for 1000 minutes, the Laves phase transformation had not reached equilibrium and was still continuing. This indicates that although the chemical driving force for Laves phase nucleation should be relatively high at this temperature due to a high undercooling, the lowered diffusivity of Nb atoms at this temperature led to a low overall nucleation rate. Also, it was observed that at 700 °C, the transformation kinetics of the Laves phase are much higher than those of the specimens annealed at higher temperatures of 750 °C and above, i.e. the volume fraction of Laves phase was observed to be much higher at 700 °C than with any other specimen annealed at higher or lower temperatures. This already hints at the possibility of a second lower temperature nose in a TTT diagram for this phase. The same observation was made by Sawatani et al [8], on the Ti and Nb stabilised low C, N – 19%Cr – 2%Mo stainless steel, where they have observed the Laves phase precipitates to be in a far larger quantity after annealing at about 700 °C. At 850 °C in Figure 8.1, the volume fraction of the Laves phase precipitates in Steel A reached a maximum of only 0.005 %, and a proper S-curve could not be established. However, this already shows a discrepancy between the experimental evidence of 0.005% volume fraction remaining at 850 °C versus the Thermo-Calc® prediction that no Laves phase should be present at and above about 825 °C in this Steel A.

8.3 LAVES PHASE TRANSFORMATION KINETICS

The kinetics of an isothermal transformation is usually expressed by the modified *Johnson–Mehl–Avrami–Kolmogorov* (*JMAK*) type of equation:

$$V_v = 1 - \exp\left(-kt^n\right) \qquad \text{Equation 8.1}$$

where V_v is the Laves phase volume fraction, k is the reaction rate constant, and n is the time exponent. From Figure 8.1, the points that fall between 5 and 95 percent on the S- curves (on the specimens annealed in the temperature range of 700 – 825 °C) were used to determined the evolution of the Laves phase by plotting them in the $\{ln\ln [1/(1-V_v)]\}$ vs $\{ln\ t\}$ relationship, see Figure 8.2. The results produced a linear relationship with the slope n and intercept $ln\ k$, and the calculated values are shown in Table 8.1. The time exponent values of n were found to range between 1.48 and 1.54, with n at 800 °C the lowest with n = 1.37. The results suggest that Laves phase nucleation takes place on either plane or edge grain boundaries [108].

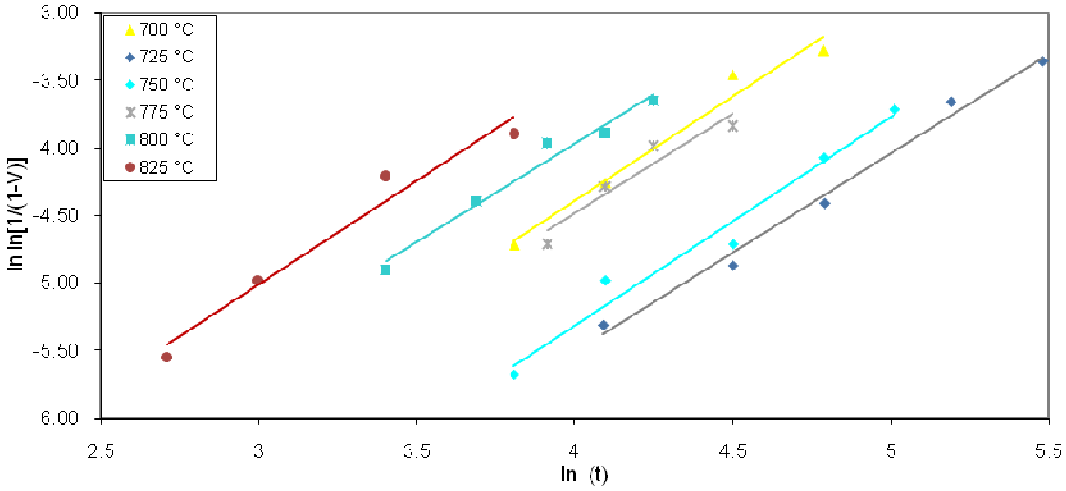

Figure 8.2. The Laves phase transformation curves according to the Johnson–Mehl–Avrami–Kolmogorov (JMAK) type of equation.

Table 8.1. The measure values of the time exponent *n* and the rate constant *k*, obtained from the best fit equation of the plots in Figure 8.2.

Temp (°C)	Best fit eqn	R^2	n	ln k	k
700	y=1.54x – 10.54	0.97	1.54	-10.54	2.65E-05
725	y=1.48x – 11.42	0.99	1.48	-11.42	1.10E-05
750	y=1.48x – 11.23	0.99	1.48	-11.23	1.33E-05
775	y=1.48x – 10.40	0.91	1.48	-10.40	3.04E-05
800	y=1.37x – 9.64	0.98	1.37	-9.64	8.54E-05
825	y=1.54x – 9.61	0.96	1.54	-9.61	6.69E-05

The activation energy for the Laves phase was estimated from the reaction rate constant k which is temperature dependent and can be expressed as :

$$k = A\exp\left(\frac{-Q}{RT}\right) \qquad \text{Equation 8.2}$$

where A is the pre-exponentials factor, Q is the activation energy, R is the gas constant, and T is the temperature. By plotting a linear relationship of *ln k vs 1/T,* the activation energy for the Laves phase precipitation was determined as the slope using the following relationship:

$$Q = -R\left(\frac{\partial \ln k}{\partial \frac{1}{T}}\right) \qquad \text{Equation 8.3}$$

and Q was estimated to be 211.3 kJ/mol, a value that is somewhat lower than the activation energy for the diffusion of Nb in a ferrite matrix, which was estimated to be about 240 kJ/mol [103]. It should be noted that this measurement of the activation energy was carried out using only data from the temperature range of 750 to 825 °C as it appears that the precipitation mechanism may be different at lower temperatures than that in this temperature range. If all the data points from all temperatures were used the activation energy was estimated to be much lower, only about 107.5 kJ/mol, possibly suggesting the introduction of enhanced diffusion along grain boundaries into the kinetics.

8.4 Temperature Effect on Isothermal Transformations

The kinetics of the Laves phase transformation were found experimentally at a number of different constant temperatures, and this led to a complete isothermal transformation diagram being drawn. Figure 8.3 is a time – temperature – precipitation (*TTP*) diagram for the Laves phase formation, and it gives the relation between the temperature and the time for the fixed fractions of transformation to be attained. Three of these curves are given in the *TTP* diagram, for the measuring times ($t_{5\%}$ and $t_{95\%}$) for the beginning and end of transformation and for 50% transformation, i.e. $t_{50\%}$. From Figure 8.3, it should be noted that the points on the solid line were determined experimentally and the dash lines are extrapolated estimated lines.

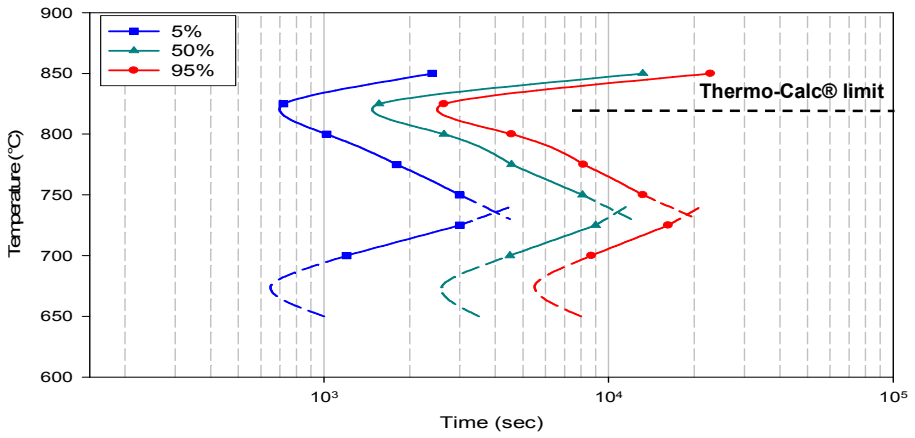

Figure 8.3 A time – temperature – precipitation (TTP) diagram for the Laves phase formation in Steel A.

The results show two classical C noses on the transformation curves, the first one occurring at a higher temperature of about 825 °C and the second one at much lower temperatures, estimated to possibly be in the range of about 650 to 675 °C. Because of extraordinary long annealing times due to the much slower diffusion, it was found to be impractical to find the exact point of this lower temperature nose. The available results, however, are sufficient to show that there are probably two types of the Laves phase transformations controlled by different nucleation mechanisms that are taking place in this steel. In the work done by Silva et al. [133] on the AISI 444 ferritic stainless steel (that is, similar to Steel E from this work, but slightly different in composition), the authors have also estimated the C nose of the transformation curve to be around 800 to 850 °C. Thermo-Calc® predictions on this Steel A have estimated the solvus temperature of the Laves phase to be 825 °C, but the experimental results indicate that the Laves phase still exists up to the temperature of 850 °C or even more.

8.5 Effect of the Grain Size on the Transformation Kinetics of Laves Phase

The transformation kinetics of the Laves phase were compared in two specimens from Steel A with different grain sizes, with the objective to evaluate the effect of grain size on the formation of the Laves phase precipitates in this AISI type 441 ferritic stainless steel. The materials were first annealed at the temperatures of 850 °C and 950 °C for 2 hours and then water quenched. The corresponding linear intercept grain sizes were determined to be 49.9 μm and 152.1 μm, respectively from which the grain boundary surface areas per unit volume S_v were calculated to be 4.008×10^4 and 1.315×10^4 m^2/m^3 respectively, i.e. a difference of 67% in the potential nucleation site availability

for grain boundary nucleation. Subsequently, the specimens were annealed at 750 °C for different periods in order to determine the Laves phase transformation kinetics. Figure 8.4 show the two typical S – shaped transformation curves obtained from the XRD analyses. The results show that the precipitation kinetics of the Laves phase is retarded by the large grain size, and this is due to a smaller number of nucleation sites. However, it was observed that an equal level of the maximum volume fraction could be achieved from both grain sizes, although at different annealing times. Within the specimen with a larger grain size the same volume fraction of Laves phase precipitates could be achieved but by annealing for approximately an extra 400 minutes. It is revealing to note that the difference in time to achieve the 50% transformation level in Figure 8.4 is reasonably close to the earlier 67% difference in the grain boundary nucleation site availability. These results confirm that grain boundary nucleation of the Laves phase's nuclei is of overriding significance. In a similar study done by Pardal et al. [134] on a superduplex stainless steel UNS S32750, the authors have made similar qualitative observations, but they did not determine the overall effect of the grain size on the volume fraction as was done here.

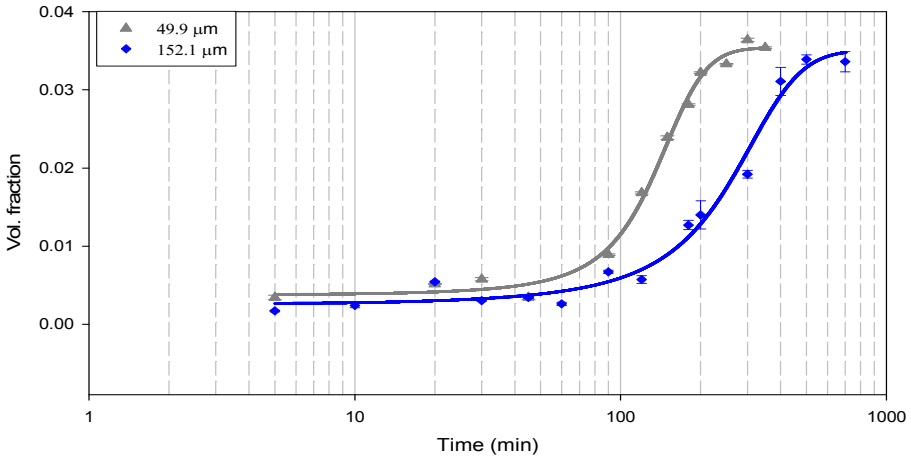

Figure 8.4. Effect of the grain size on the Laves phase kinetics transformation in Steel A. The specimens were annealed first at 850 and 950°C respectively to set different grain sizes and were then annealed both at 750 °C for different annealing periods.

8.6 Effect of the Steel's Composition on the Laves Phase's Transformation Kinetics

The effect of the steel's composition on the Laves phase kinetics was investigated comparing Steel A (0.444Nb – 0.153 Ti – ~ 0Mo), with the Steel C (0.36Nb – 0.171Ti –<

0.01Mo) and Steel D (0.251Nb – 0.106Ti – 1.942Mo). The grain size of these materials was kept constant and the transformation kinetics was investigated by annealing the specimens at 750 °C over different periods of time. Figure 8.5 shows the results of the effect of composition on the kinetics of the Laves phase precipitation, which indicates that at 750 °C, Steel A has a much higher volume fraction of Laves phase precipitates than Steels C and E, and this coincides with the Thermo-Calc® predictions. Note that from Figure 8.5, in order to be able to compare the volume fractions of Laves phase of Steels C and E, their smaller values are shown on the secondary axis while that of Steel A is shown on the primary axis.

These results also indicate that by reducing the Nb and Ti contents as with Steel C (in comparison to Steel A), this did not have any significant impact on the kinetics of the Laves phase precipitation but only on the final volume fraction. But the addition of 1.942% Mo has a measurable impact by retarding the precipitation rate of the Laves phase. In the work published by Ahn et al. [135] the authors have observed that the precipitation of Fe_2Nb Laves phase in 0.01C–0.38Nb–1.2Mo steel was slower than in an 0.01C-0.38Nb steel, and this was due to Mo retarding the rate of Nb diffusion.

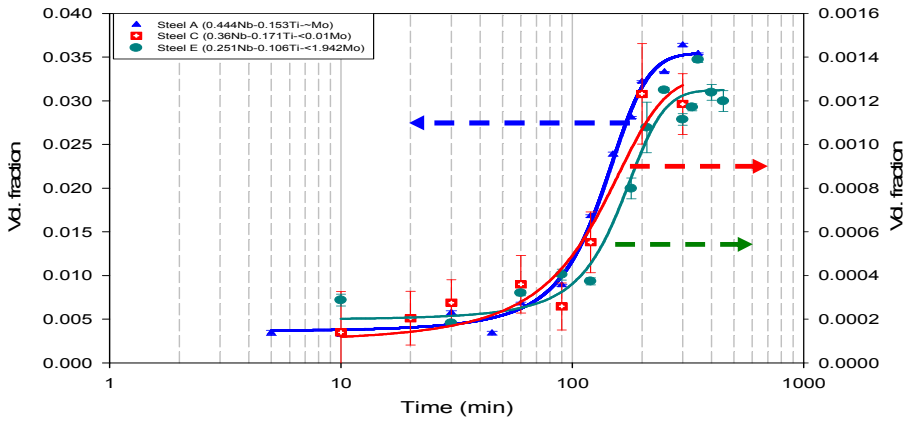

Figure 8.5. Effect of the steel's composition on the Laves phase transformation kinetics. The specimens from these steels were all annealed at 750 °C for different annealing periods.

8.7 Microstructural Analysis of the Transformation Kinetics

The nucleation mechanisms of the Laves phase precipitates during transformation was investigated from the specimens that were annealed at 600 °C, 750 °C and 800 °C for 30 minutes, which allowed for a suitable time of precipitate growth, so that they could be analysed using TEM – EDX.

Figure 8.6, shows the microstructure of the specimen annealed at 600 °C. At the lower magnification (Figure 8.6(a)) the remnant of the grain boundary Laves phase precipitates could be found from the solution treatment at 850 °C for 2 hours. At a higher magnification (Figure 8.6(b), the same area analysed from Figure 8.4 (a) is indicated by a circle, and the micrograph indicates that the nucleation site for the Laves precipitation is mainly at dislocations and subgrain boundaries, with only a very few precipitates on grain boundaries and almost none within the grains themselves. Laves phase precipitates that have nucleated on the grain boundaries, are possibly coherent or alternatively have a low mismatch with one grain but grow into the adjacent grain with which they do not have a rational orientation relationship because of that interface's higher mobility. Similar observations were made by Li [131] on 12Cr – 2W steel, where it was found that with the nucleation and growth of the Fe_2W Laves phase precipitates, the coherent or low mismatch interfaces have a low mobility while the incoherent ones have a higher mobility, and therefore, the incoherent interface will grow into the grain with which there is no rational orientation relationship.

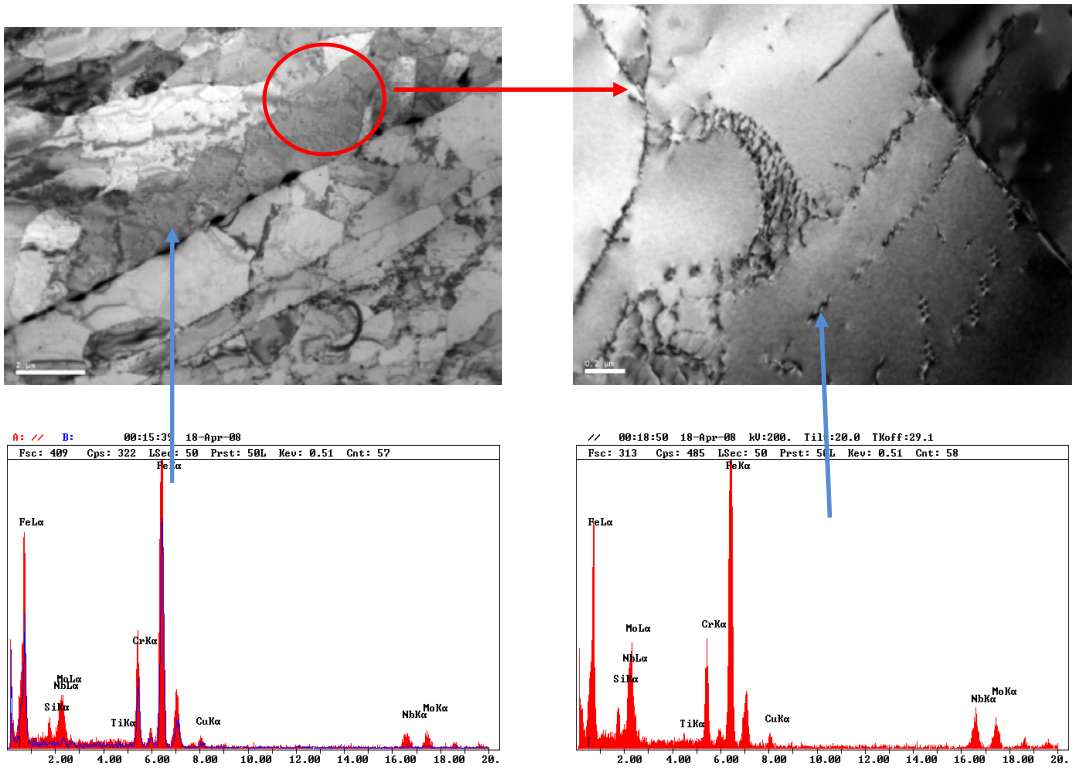

(a) **(b)**

Figure 8.6. TEM micrographs of the specimen of Steel A annealed at 600 °C; (a) a low magnification micrograph shows coarse grain boundary Laves phase precipitates, and (b) the same area but at a high magnification, showing Laves phase precipitates nucleated on subgrain boundaries and dislocations.

The microstructure of the specimen of Steel A that was annealed at 700 °C is shown in Figure 8.7. Comparing this specimen with the one that was annealed at 600 °C, it can be seen that even after only 30 minutes of annealing, the volume fraction of the Laves phase is higher, also suggesting a high nucleation rate at 700 °C in this specimen. Also, there is more of the grain boundary Laves phase precipitation than the dislocation precipitates, see Figure 8.7 (a). This suggests that the most preferred nucleation site for the Laves phase are the grain and subgrain boundaries, unlike as in the specimen annealed at 600 °C, where more precipitates on dislocations were observed.

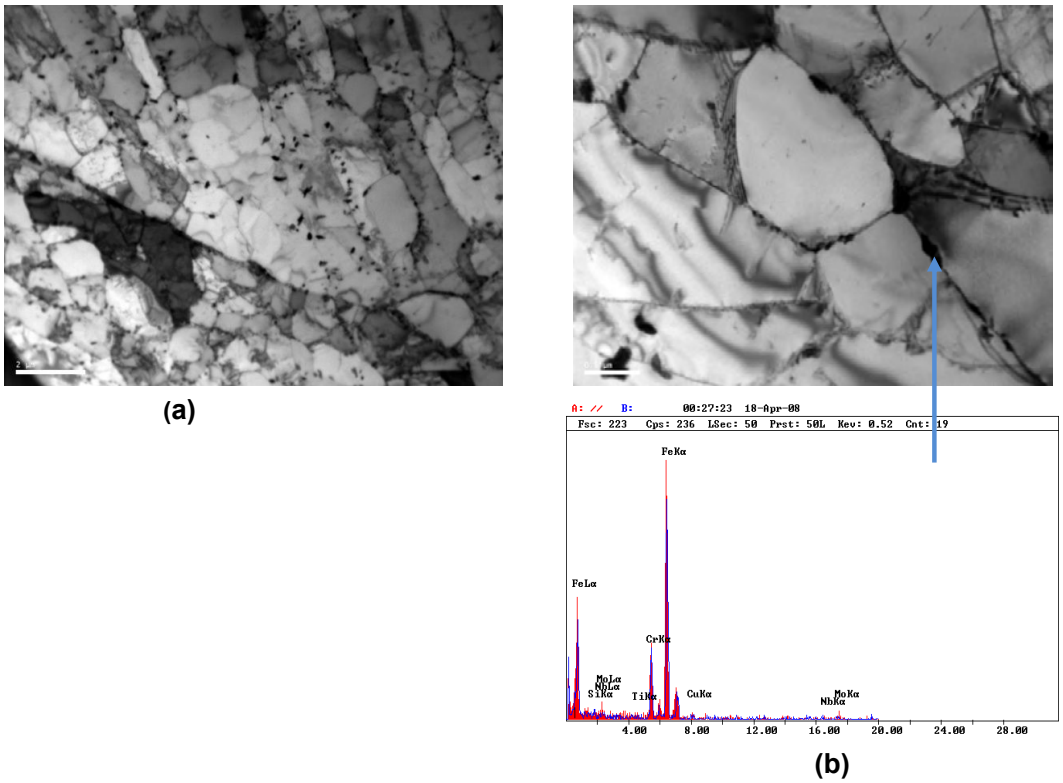

Figure 8.7. TEM micrographs of the specimen of Steel A annealed at 750 °C; (a) a low magnification micrograph showing grain and subgrain boundary Laves phase precipitates, and (b) at a high magnification, showing Laves phase precipitates nucleated on the subgrain boundaries.

Figure 8.8 shows the micrographs of the specimen that was annealed at 800 °C, which is heavily "decorated" with the Laves phase precipitates. At the higher magnification, it was observed that the preferred sites for the Laves phase nucleation are grain boundaries, with very few precipitates on dislocations compared to the specimen annealed at 600 °C. Also, it can be observed that the presence of the dislocation

density did not assist as much as preferred nucleation sites for the Laves phase precipitation as was the case at lower temperatures.

Comparing all of the microstructures at these three different temperatures, it can be concluded that dislocations, subgrain and grain boundaries act as preferred nucleation sites for Laves phase precipitation. Analyses of the microstructures and also on the basis of the classical heterogeneous nucleation theory, demonstrates that nucleation on the grain boundaries is dominant at the higher testing temperatures of 750 °C and above, see Figure 8.7 and Figure 8.8, where the undercooling and hence the driving forces for nucleation are relatively low and the system then lowers its retarding forces through grain boundary nucleation. As the temperature is decreased and the undercooling and hence the driving forces are higher, however, heterogeneous nucleation on dislocations becomes more significant.

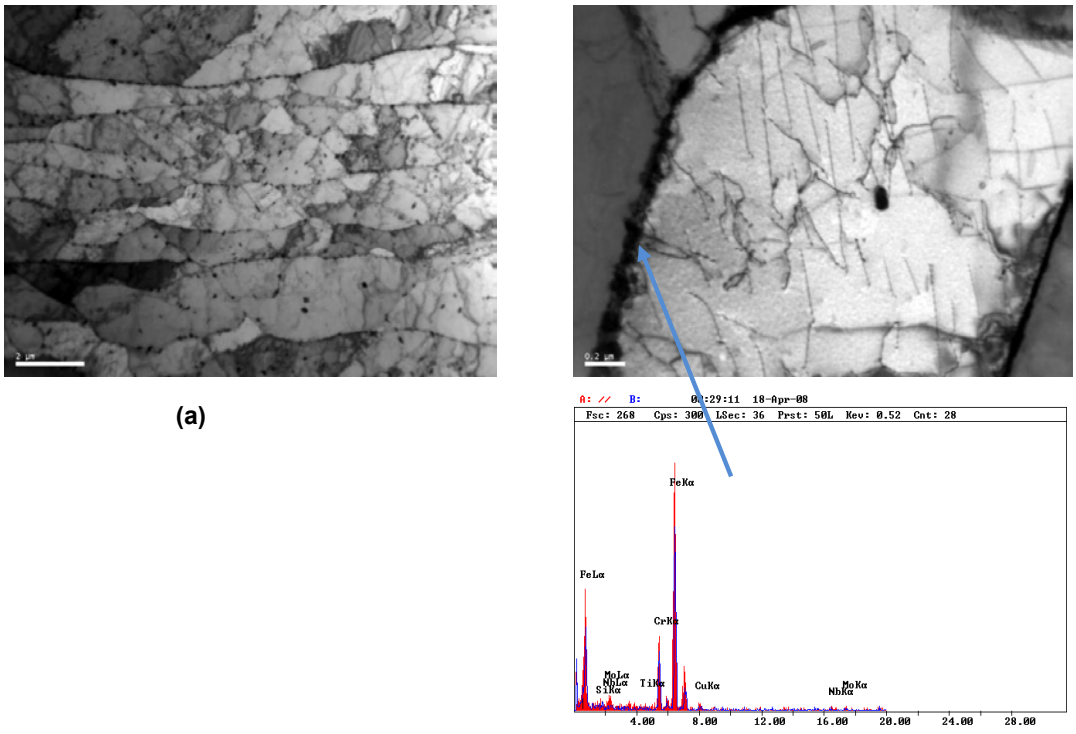

Figure 8.8. TEM micrographs of the specimen annealed at 750 °C; (a) at a low magnification, showing grain boundary Laves phase precipitates, and (b) at a higher magnification showing Laves phase precipitates nucleated on the subgrain boundaries.

8.8 ORIENTATION RELATIONSHIP BETWEEN THE LAVES PHASE AND THE FERRITE MATRIX

Figure 8.9 to Figure 8.11 show bright field images and the corresponding selected area diffraction patterns (SADP) from the Steel A specimens annealed at 600 to 800 °C, for 30 minutes. The microstructure consists of a number of differently shaped particles ranging from needle-shape at 600 °C, globular-shaped at 750 °C and plate–like at 800 °C. These precipitates were all identified as Fe_2Nb Laves phase with a C14 crystal structure.

Figure 8.9 shows the specimen of Steel A that was annealed at 600 °C and the crystallographic orientation relationship between the needle-like Laves phase and the matrix was analysed using the SAD pattern as:

$$(21\bar{1})_{\alpha-Fe} \,//\, (\bar{1}101)_{Fe2Nb} \text{ and } [011]_{\alpha-Fe} \,//\, [1\bar{1}02]_{Fe2Nb}. \quad (1)$$

According to Cocks and Borland [90], by rotating the above orientation relationship (1) to within ±5° around the habit plane $\{111\}_{\alpha\text{-Fe}}$ and a direction in this plane, the following orientation relationship is found;

$$(1\bar{1}1)_{\alpha-Fe} \,//\, (11\bar{2}0)_{Fe2Nb} \text{ and } [121]_{\alpha-Fe} \,//\, [0001]_{Fe2Nb}. \quad (2)$$

The needle-like Laves phase particles found in this specimen are, therefore, elongated in the $\langle 112 \rangle$ matrix directions.

Figure 8.10 shows the specimen that was annealed at 750 °C, in which the crystallographic orientation relationship between the globular-like Laves phase and the ferrite matrix was analysed to be the following orientation relationship:

$$(211)_{\alpha-Fe} \,//\, (0001)_{Fe2Nb} \text{ and } [\bar{1}11]_{\alpha-Fe} \,//\, [01\bar{1}0]_{Fe2Nb} \quad (3)$$

According to Yamamoto et al.[91], using the stereographic projection of the orientation relationship (1) between the Laves phase and the ferrite matrix, they have found that this orientation relationship is equivalent to the following expression by the lower mirror indices;

$$(211)_{\alpha-Fe} \,//\, (0001)_{Fe2Nb}, \text{ and } [0\bar{1}1]_{\alpha-Fe} \,//\, [\bar{2}110]_{Fe2Nb} \quad (4)$$

Figure 8.11 shows the specimen that was annealed at 800 °C, in which the crystallographic orientation between the plate-like Laves phase and the ferrite matrix was analysed to follow the orientation relationship:

$$(110)_{\alpha-Fe} \,//\, (0001)_{Fe2Nb} \text{ and } [\bar{2}33]_{\alpha-Fe} \,//\, [11\bar{2}0]_{Fe2Nb} \quad (5)$$

If the orientation relationship (5) is rotated by ±5° from the above mentioned relationship, it will follow:

$$(110)_{\alpha-Fe} \,//\, (0001)_{Fe2Nb} \text{ and } [001]_{\alpha-Fe} \,//\, [1\bar{2}10]_{Fe2Nb} \quad (6)$$

The habit plane from this orientation relationship is $\{110\}_{\alpha\text{-Fe}}$, and the preferred growth orientation must be in the $\langle 001 \rangle$ matrix directions.

Comparing all three of these SAD patterns, it can be seen that the orientation relationship between the Laves phase particle and the ferrite matrix may have a significant effect on the shape of the particles. Also, the orientation relationships for the particles analysed are completely different from one another, and the habit planes are also different.

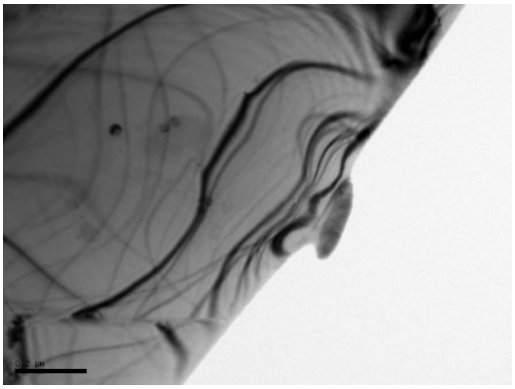

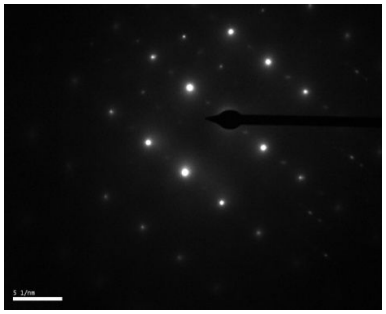

$$[011]_{\alpha-Fe} \,//\, [1\bar{1}02]_{Fe2Nb}$$

Figure 8.9. Transmission electron micrographs and corresponding selected area diffraction (SAD) pattern from Steel A annealed at 600 °C.

$$[\bar{1}\,11]_{\alpha-Fe} \,//\, [01\,\bar{1}\,0]_{Fe_2Nb}$$

Figure 8.10. Transmission electron micrographs and corresponding selected area diffraction (SAD) pattern from Steel A annealed at 750 °C.

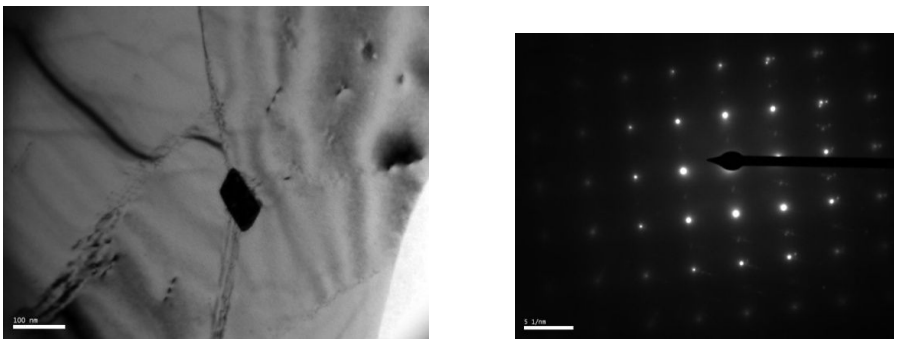

$$[\bar{2}33]_{\alpha-Fe} \,//\, [11\bar{2}0]_{Fe_2Nb}$$

Figure 8.11. Transmission electron micrographs and corresponding selected area diffraction (SAD) pattern from Steel A annealed at 800°C.